

## CHAPTER X

### Modification of layered oxide cathode materials

J. Dong<sup>a</sup>, M. Hietaniemi<sup>a</sup>, J. Välikangas<sup>b</sup>, T. Hu<sup>a</sup>, U. Lassi<sup>a,\*</sup>

<sup>a</sup> University of Oulu, Department of Sustainable Chemistry, P.O.Box 4000, FI-90014 University of Oulu, Finland

<sup>b</sup> University of Jyväskylä, Kokkola University Consortium Chydenius, Talonpojankatu 2B, FI-67100 Kokkola, Finland

\* Corresponding contributor. Prof. Ulla Lassi, ulla.lassi@oulu.fi

This is the peer reviewed version of the following article, which has been published in final form at <http://dx.doi.org/10.1039/9781788016124-00044>.

## **Abstract**

Layer-structured cathode materials for lithium-ion batteries are considered. These materials, such as LCO, NCM, NCA, lithium rich cathode oxides and blended cathodes are well-known for the intercalation mechanism. Future of lithium-ion batteries is also strongly based on these cathode chemistries, but to overcome some drawbacks and challenges, the improved materials are needed. In this chapter, modification of layer-structured cathode materials by doping and coating are discussed. Especially, coating materials and doping methods are considered.

## 1. Introduction

Layered cathode materials are one group of lithium-ion battery cathode materials characterized by a specific structure consisting of alternating layers of lithium ions and a metal compound, such as metal oxide. A layered structure is well suitable for the intercalation mechanism, where lithium ions are reversibly inserted into and removed from the host structure.

The history of layer structured cathode materials goes back to early 1970s when electron-donating molecules and ions were discovered to be able to reversibly intercalate into the layered dichalcogenides such as tantalum disulfide and titanium disulfide. Exxon commercialized coin cells using LiAl anodes and  $\text{TiS}_2$  cathode in 1977-1979.<sup>1</sup> Layered oxides, the cousin of dichalcogenides, gained their attention shortly thereafter.  $\text{LiCoO}_2$ , introduced by J. B. Goodenough<sup>2</sup>, was the first layered transition metal oxide used in commercial lithium-ion batteries, and has since become the most common cathode material for rechargeable batteries.<sup>3</sup>

Different variations of layered transition metal oxides have since been studied in order to enhance the performance of lithium-ion batteries. Recently the rising cost of cobalt has been driving battery manufacturers to replace it with a cheaper alternative. Many of the alternative materials are isostructural to  $\text{LiCoO}_2$ , such as  $\text{LiNiO}_2$  and  $\text{LiMnO}_2$  all of them having  $\alpha\text{-NaFeO}_2$  structure. These substitutions of cobalt solve some problems of  $\text{LiCoO}_2$  regarding to cost and toxicity as nickel and manganese are cheaper and less toxic than cobalt, but both  $\text{LiNiO}_2$  and  $\text{LiMnO}_2$  have problems with structural instability during charge-discharge cycling, leading to structural collapse or metal dissolution. This has led to the introduction of a group of materials called mixed metal oxides. The idea is to minimize the bad effects of all materials while also retaining the good properties. One common type of mixed metal oxide, NCM333 first introduced by Ohzuku et al. in 2001<sup>4</sup>, has a mix of cobalt, nickel and manganese in equal amounts. The metals form a solid solution, meaning that they occupy random, interchangeable spaces in the structure. A wide range of NCM materials with different metal ratios has been developed since then. Another commercialized layer structured mix metal oxide is NCA, where the metals are nickel, cobalt and aluminium.

A reasonable next step from mixed metal cathodes, is the doping of cathodes. The difference between a mixed metal oxide and a doped oxide is vague, but generally the amounts used in doping are around 5 % of metal content, whereas in mixed metal cathodes each metal is upwards of 10 %.

The most important goal of doping layered cathode materials is to improve stability of cathode in its delithiated state. This would allow for a larger portion of the Li<sup>+</sup> ions to be removed safely and would therefore increase the capacity of the material. Doping with a small amount of different metals can affect the electronic structure in a way that stabilizes the material, and can prevent structural collapse during lithium removal. Doping can also affect other characteristics, such as volume change during cycling, Li-ion diffusion, etc. The small amounts used might allow for some of the more exotic metals to be considered as dopants.

Another method of modification for cathode materials is coating. Coating differs from doping in that the coating is mainly meant to prevent interaction between electrolyte and the cathode material. Usually coating is the last ditch effort to make otherwise unusable material able to function in a cell, much like the SEI-layer (solid-electrolyte interphase) is crucial to the functioning of a graphite anode. Coating has become increasingly important and common as the potential voltage of cathodes has risen to levels that organic solvent based electrolytes cannot withstand without decomposing ( $\sim 4.5$  V). CEI-layers (cathode-electrolyte interphase) from electrolyte additives are coming along also<sup>5</sup>, but coating is used because of its simplicity.

In short, layered cathode materials are in the near future the only cathode materials that have the product qualities expected by consumers, are known to function, have commercial production capability and know-how to be quickly utilized.  $\text{LiCoO}_2$  has drawbacks such as the high cost of cobalt, yet the advantages are also obvious, for example easy synthesis and high cycling capability. It is still widely used cathode material for lithium-ion batteries and the layered derivatives make up most of the rest. Layered materials can be further optimized with mixed metals, doping and coating, to achieve good cycling behavior, high voltage, high power and moderate cost. This chapter focuses on the doping and coating of layered materials. Notice that this chapter only addresses layer structured materials, not for example spinel types that are a separate type of cathode materials, and the optimization of transition metal ratios is addressed in another chapter.

## 2. Common layer-structured materials

This section more closely introduces the most common layered oxide cathode materials, their structure and the problems that need to be addressed by modification.

### 2.1 LCO

$\text{LiCoO}_2$  has the  $\alpha\text{-NaFeO}_2$  structure (**Error! Reference source not found.**), where  $\text{CoO}_6$  octahedra share edges to form layers of  $\text{CoO}_2$ . In its uncharged state Li-ions are intercalated between the layers of  $\text{CoO}_2$  and form an alternating layered structure. Li-ions and Co-ions are both located in octahedral sites, so the structure can be also considered as layers of  $\text{CoO}_6$  octahedra and layers of  $\text{LiO}_6$  octahedra that share edges and stack on each other alternatively. The structure of  $\text{LiCoO}_2$  allows rather high Li-ions charge/discharge rate and small volume changes upon intercalation and de-intercalation of Li ions. The interlayer distance changes from 4.68 Å at fully lithiated state to 4.24 Å at fully delithiated state.<sup>7</sup>

[Figure 1 close here]

$\text{LiCoO}_2$  was used in the first commercial lithium-ion batteries due to its simple synthesis, good cyclability, high operating voltage and is still commonly used in modern lithium-ion batteries.<sup>8</sup> For  $\text{LiCoO}_2$  the reaction of lithium de-intercalation can be expressed as:



The capacity of cathode material is determined by the amount of lithium ions that can be removed reversibly.  $\text{Li}^+$  removal is always accompanied by loss of  $e^-$ , this is the basic functioning principle of a lithium ion battery. The ability of  $\text{LiCoO}_2$  to intercalate lithium reversibly is due to cobalt being a transition metal, which means that it has several stable oxidation states that are relatively close in energy. The voltage at which Li removal happens is related to the ability of the transition metal to oxidize. When  $\text{LiCoO}_2$  is delithiated (charged), the oxidation state of cobalt ions in the material will increase gradually from +3 to +4 as the Li-ion content in  $\text{LiCoO}_2$  drops from 0,8 to 0,45. The redox reaction between  $\text{Co}^{3+}$  and  $\text{Co}^{4+}$  offers a high discharge voltage up to 4.2 V (vs  $\text{Li}^+/\text{Li}$ ). Theoretical capacity of  $\text{LiCoO}_2$  is 247 mAh/g. However, only half of the Li-ions can be de-intercalated safely without severe structural damage and oxygen release. This is usually stated as  $x < 0.5$  in Equation 1. When more than half of Li is extracted, in addition of the Co-ions giving away electrons, electrons in oxygen 2p orbitals are also removed due to the overlap of oxygen 2p orbital and Co  $t_{2g}$  (3d) orbital. As a result,  $\text{O}^{2-}$  is oxidized into  $\text{O}_2$  gas. It is also found that when more Li-ions are extracted, more cobalt is dissolved in the electrolyte, which causes severe damage to the stability of the structure, and puts a limit to  $\text{LiCoO}_2$  at a relatively low practical capacity of 130-140 mAh/g. This has been enough for small portable devices, but for EVs (electric vehicle) the capacity per gram needs to be higher in order to provide enough charge for long distances without increasing the weight and size of the battery too much.

Low thermal stability is also a major problem of  $\text{LiCoO}_2$ . When heated to a certain temperature, oxygen released from  $\text{LiCoO}_2$  reacts with organic materials such as electrolyte in the battery, the exothermic reaction creates a thermal runaway.<sup>9</sup> Micro crack formation is a known problem in layered materials that arises from the c-lattice parameter shrinking and growing when lithium ions are intercalated into and removed from the structure (c parameter is the one perpendicular to the lithium-ion and transition metal oxide layers). Cobalt compounds are also toxic, which means that care has to be taken with handling and storage of the batteries. All of these concerns can be mostly dealt with by limiting the upper charge voltage and having external battery management and safety systems. The ultimate death blow to  $\text{LiCoO}_2$  cathodes will be the increasingly high price and limited availability of cobalt.

## 2.2 NCM

NCM refers to a group of materials which are solid solutions of nickel, cobalt and manganese oxide in different molar ratios. The molar ratios are marked with three numbers after the letters, each giving the molar percentage given in the subscripts of the chemical compound, e.g.  $\text{LiNi}_{0,8}\text{Co}_{0,1}\text{Mn}_{0,1}\text{O}_2$  is marked NCM811. NCM combines the advantages of  $\text{LiCoO}_2$ ,  $\text{LiNiO}_2$  and  $\text{LiMnO}_2$ . Cobalt, nickel and manganese provide synergistic effects for the cathode material. The electrochemical and physical properties of the material vary with different transition metal ratios. All the above mentioned NCM cathode materials have the same  $\alpha\text{-NaFeO}_2$  layered structure as  $\text{LiCoO}_2$ , but part of cobalt is substituted by nickel and manganese.

A clear signal from battery and EV industry for cathode material is to go high nickel. The trend is driven by the ever-increasing cobalt price. Commercially available  $\text{LiNi}_{1/3}\text{Co}_{1/3}\text{Mn}_{1/3}\text{O}_2$  and  $\text{LiNi}_{0.5}\text{Co}_{0.2}\text{Mn}_{0.3}\text{O}_2$  no longer fill the need of low cost and high performance, so  $\text{LiNi}_{0.6}\text{Co}_{0.2}\text{Mn}_{0.2}\text{O}_2$  and  $\text{LiNi}_{0.8}\text{Co}_{0.1}\text{Mn}_{0.1}\text{O}_2$  have gained the attention. According to the metal ratios, those NCM cathode materials are also known as 333 (interchangeably called also NCM111), 523, 622 and 811 respectively.

Ni has lower oxidation potential than Co. This means that more of the capacity can be utilized without raising the potential, which is observed as improved discharge capacity. Nickel enhances the energy capacity but harms the cyclability and stability due to Ni-O bonds being weaker than Co-O bonds.  $\text{Ni}^{2+}$  ions are notoriously mobile in the layered cathode structure, and nickel rich materials can have a high degree (~10%) of cation mixing, where  $\text{Ni}^{2+}$  occupies  $\text{Li}^+$  sites. Cation mixing leads to capacity drop and high cation mobility makes the layer to spinel transformation easier, leading to shorter cycle life and lower thermal resistance for nickel rich materials. Pure  $\text{LiNiO}_2$  is not usable as a cathode material because it gives very poor cyclability and is known to be dangerously vulnerable to thermal runaway. Cobalt can inhibit these negative effects by preventing nickel atoms from entering lithium sites. The introduction of manganese into the material brings down the production cost and improves the safety of the material by stabilizing the structure. However, manganese also decreases the capacity because in layered structure Mn stays fully oxidized as  $\text{Mn}^{4+}$  and has no contribution to the discharge capacity.<sup>10,11</sup> Because of this, Mn could be considered a dopant in layered structure. Increasing Mn content overtly will also destroy the layered structure, because manganese with its multiple oxidation states will prefer  $\text{LiMn}_2\text{O}_4$  spinel structure instead of layered  $\text{LiMnO}_2$  structure.

With high nickel content, the discharge capacity is increased. NCM811 can deliver a discharge capacity of 200 mAh/g in the voltage range of 3.0-4.3 V at 0.1 C rate in first 60 cycles.<sup>12</sup> With same charge discharge conditions (voltage and discharge rate), the reversible discharge capacity of 333, 523, 622 and 811 materials increases with the increase of nickel content. However, the cyclability is worse with higher nickel content materials. The relationships are illustrated in Figure 3. Currently the main research focus on NCM materials is to optimize the transition metal ratio to reach the point where the pressure from costly cobalt and requirements for the electrochemical properties can be balanced.

[Figure 2 close here]

## 2.3 NCA

Like NCM, NCA could be considered a solid solution of  $\text{LiNiO}_2$ ,  $\text{LiCoO}_2$  and  $\text{LiAlO}_2$ . NCA is another compromise between the better capacity but poorer safety of  $\text{LiNiO}_2$  and better stability but higher price of

LiCoO<sub>2</sub>, with added structural stability coming from electrochemically inactive aluminium instead of manganese. NCA is also a nickel rich cathode material, with nickel/cobalt ratio from 7/3 up to 9/1. Generally, nickel is over 80% of all the metal content. As in NCM, higher Co content improves thermal stability because cobalt prevents nickel from moving into the lithium layer. Higher Ni content means higher initial capacity, however, the capacity of the cell fades away very quickly because of the rise of the cell impedance (low electronic conductivity). Aluminum doping has proved to be a good way to suppress the impedance. This Al-doped LiNiCoO<sub>2</sub> has become a very commonly used cathode material.<sup>13-15</sup> The cylindrical cells in Tesla Model S use NCA cathodes, which provides a driving range of 480 km on a single charge. Specific capacity of NCA cathode material can reach 180-200 mAh/g.<sup>3</sup>

The issues of NCA are very similar to high nickel NCM. One of them is that in LiNi<sub>0.8</sub>Co<sub>0.15</sub>Al<sub>0.05</sub>O<sub>2</sub>, Ni<sup>2+</sup> occupies Li<sup>+</sup> sites due to the similarity in radii, which causes capacity loss during charge and discharge. Also, side reactions between Ni<sup>4+</sup> and electrolyte releasing oxygen and heat cause safety problems. The storage life of the material is also harmed by the basicity of the LiNiO<sub>2</sub> which makes it easily react with CO<sub>2</sub> and H<sub>2</sub>O in the ambient environment.

## 2.4 LLO and blended cathodes

Lithium rich layered oxides (LLO) are the newest type of layered cathode material, first reported in 2000 by Paulsen et al.<sup>17</sup> Sometimes LLOs are called composite cathodes because they can be thought of as a mixture of transition metal oxide and manganese spinel, though evidence shows that at least sufficiently over lithiated samples are not a mixture of two phases, but instead actually solid solutions with large amount of crystal defects.<sup>16</sup> Most simple way to compare them to traditional layered materials is to think of them as layered transition metal oxides but with lithium replacing a transition metal in the transition metal layer in regular pattern, in addition to having lithium in the lithium layer (Figure 4). LLOs can be based either on high manganese content materials with chemical composition Li[Ni<sub>x</sub>Li<sub>(1/3-2x/3)</sub>Mn<sub>(2/3-x/3)</sub>]O<sub>2</sub><sup>18</sup> or nickel materials such as Li[Li<sub>1/3</sub>Ni<sub>2/3</sub>]O<sub>2</sub><sup>19</sup>. Newer materials with some cobalt in the structure were introduced by Thackeray et al.<sup>20</sup> in 2007 and have better stability. Some of these lithium-rich NCMs such as Li[Li<sub>0.2</sub>Ni<sub>0.13</sub>Co<sub>0.13</sub>Mn<sub>0.54</sub>]O<sub>2</sub> or Li<sub>1.17</sub>Ni<sub>0.19</sub>Co<sub>0.10</sub>Mn<sub>0.54</sub>O<sub>2</sub> are commercially available as HE-NCM (high energy NCM). Manufacturing LLOs can be done via co-precipitation similar to traditional layered oxides.

[Figure 3 close here]

LLOs are particularly interesting materials, because in some cases capacities that are “over theoretical” are observed. This is possible because in addition to transition metal oxidation, the oxygen atoms participate in the redox reactions during charge-discharge. Li-O-Li bonds can leave O2p orbitals unhybridized (meaning they are not in a bond). These non-bonding electrons can contribute to charge compensation. Whether they do, is also dependent on the transition metals in the material. Transition metals that are in their highest oxidation state and are hard to oxidize further, such as Mn<sup>4+</sup> and Zr<sup>4+</sup>, promote oxygen participation. If this

oxygen oxidation (more correctly called electron vacancy on the oxygen atoms) is reversible, it increases the materials useable capacity. The oxygen oxidation can also be irreversible, in which case it leads to capacity loss and oxygen evolution:



While anionic oxygen has been observed to participate in for example LCO, in lithium-rich materials it can hopefully be utilized reversibly.<sup>21,22</sup>

Lithium rich materials have very high capacities (~250 mAh/g), but they also show significant discharge capacity fade during cycling, and their operating voltage is so high (>4.5 V) that it limits actual use because current electrolytes can not handle so high voltages.<sup>23</sup> Structural modification is needed to make LLOs commercially viable.

Blended cathodes are different from composite cathodes. They are a physical mixture of different layered cathode material powders, or a mixture of layered material and Mn-rich spinel made in to a single cathode foil. In blended cathodes, each material is in distinctly different particles, so the outward behavior of the cathode is a sum of all the materials. There is some evidence of structural stabilization in blended cathodes. LIBs with blended cathodes are commercially available.<sup>24,25</sup>

### 3. Modification methods

Effects that degrade battery performance during cycling can be roughly divided to two categories, external ones related to unwanted reactions with electrolyte, and internal ones that are due to structural changes during the Li-ion intercalation. (In truth this is more complicated, for example metal dissolution can be caused by structural changes, etc.) The first problem can be addressed with coating the cathode material, though strictly speaking this is also a problem with the electrolyte and can also be addressed by developing more durable electrolyte salts, using solid electrolytes or CEI-forming additives. However, coating is very easy and effective fix to an otherwise complicated problem. Internal structural problems can be addressed with doping.

In recent years, there has been an almost overwhelming wealth of studies about modified cathode materials, where some of the results are questionable. Usually these studies have a bafflingly poor “pristine” material as a comparison sample, very small differences in capacities between different samples, short cycling time, no parallel cells and some have so thin film thickness on the cathode foils that in laboratory setting it is impossible to guarantee that the loading in different samples has been equal. There are a lot of possible ways that electrochemical measurements can be influenced during making of the cell, such as bad contact, moisture, etc. Small capacity differences (5-10%) without multiple parallel cells should always be assumed to be measurement errors.

The easiest way to spot results that need to be handled with care is to be aware of the level of performance that unmodified layered cathode materials are capable of, and the effects that battery testing conditions have on the results. In Figure 5 is the cycling behavior of completely unmodified NCM622 (precipitated by us) that has been lithiated in air and cycled between 3,0-4,2 V for 1200 cycles. Lithiation in pure oxygen would give slightly better capacity in a Ni-rich sample such as this. The program starts with cycles using charging speeds of 0,03 C, 0,1 C, 0,2 C and 1C, then continues at 2 C charging and discharging rate, with checks at 0,2 C in between and in the end. As can be seen, the discharge capacity is directly proportional to the discharge speed, and c-rate should always be included when comparing capacities. What can also be seen is the breakdown of our air ventilation unit at about 590 cycles, where the laboratory room temperature rose from around 22 °C to about 30 °C. Higher temperature will give higher capacities, so samples cycled in different temperatures are not directly comparable.

This sample gave capacity retention of 93% after 1200 cycles. One of the reasons for this good cycling behavior is that the cut-off voltage is limited to 4,2 V, which is both within the electrolyte comfort zone and does not induce structural changes in the cathode material. When the cut-off voltage is raised higher, the capacity will of course also be higher. In such cases care should always be taken to demonstrate that this capacity increase is justified because of improved stability and does not come at the cost of breaking the cathode. It is also important to remember that particle size and morphology of the cathode material have effect on electrochemical properties, and different thermal and mechanical treatments may affect things like cation disorder. Physical differences between doped and undoped comparison samples should be taken in to consideration when interpreting results. In Table 1 is listed the performance of some of the common unmodified materials.

[Figure 4 close here]

[Table 1 close here]

### 3.1 Coating

Battery performance drops during cycling because transition metals react with or dissolve in the electrolyte under heavy cycling. One of the detrimental reactions in a full battery cell is the water catalyzed break-down of lithium electrolyte salt  $\text{LiPF}_6$  into HF, which then will dissolve the cathode. Another unwanted side reaction is the degradation of organic solvents in electrolyte when exposed to voltages higher than 4,2 – 4,5 V (depending on the electrolyte).<sup>29-31</sup> The idea of coating is to provide a shield that protects the cathode material from direct contact with the electrolyte.

Coating has been used on LCO<sup>32,33</sup>, NCM<sup>34</sup> and NCA<sup>35</sup>. All of them show positive results on improving electrochemical performance and stability of the material. Coating layer can inhibit undesired reactions between the electrode and the electrolyte and at the same time suppress structure distortion caused by transition metal dissolution in the electrolyte. In some cases, when the discharge voltage is high enough to cause electrolyte decomposition on the electrode surface, having a coating layer that prevents direct contact between the electrolyte and cathode reduces the influence of electrolyte decomposition on the battery performance.<sup>36</sup>

Other mechanisms include preventing the transition metal dissolution during charging and improving electron conductivity and lithium ion diffusion rate on the cathode surface. A proper coating material, with the above-mentioned mechanisms will improve largely the electrochemical performance of the cathode material as well as thermal stability related battery safety. Many factors must be taken into consideration in the surface modification such as the chemical and physical properties of both cathode and coating materials, thickness of coating material used and the coating method. These factors will determine the performance of the coating layer and affect the overall performance of the cathode material.

### 3.1.1 Coating materials

Coating materials are generally classified into metal oxides, metal fluorides and phosphates, lithium salts, carbon materials and others. Oxides like Al<sub>2</sub>O<sub>3</sub>, SiO<sub>2</sub>, SnO<sub>2</sub> etc. can provide a good barrier between the cathode material and the electrolyte and reduce the negative reactions on the interface. However, they also reduce the transportability of lithium ions as well as electrons, limiting rate performance. Lithium salts and carbon coating can increase the conductivity. In some cases, a combination of more than one coating materials is used to provide a better result.<sup>37</sup> The pre-modification of coating material is also a way to improve the low conductivity.<sup>38,39</sup>

ZnO can grow onto LCO surface easily due to their similarity in structure, which makes it a good choice of coating material for layered LCO. To provide a better electronic conductivity for the coating material, Dai et al.<sup>38</sup> coated Al<sub>2</sub>O<sub>3</sub>-doped ZnO (AZO) layer on the LCO cathode via magnetron sputtering as small amount of Al<sub>2</sub>O<sub>3</sub> doping in ZnO does not change the main constitute yet makes ZnO a conductive material. The electrochemical test of the AZO coated LCO gave positive results. A remarkably high stability in cycling performance test was observed. A reversible capacity of 173 mAh/g (90% retention rate) is maintained after 150 cycles, which was almost twice as much as the uncoated LCO. It is noted that a proper thickness of AZO coating was very important to achieve the balance between surface protection and electrochemical performance. As in their experiment, a series of thickness was tested, 20 nm gave the best result as shown in Figure 6. The 20 nm AZO coated LCO also had a better rate performance. The coated electrode exhibited considerably higher reversible capacities at all elevated rates compared to bare electrode.

[Figure 5 close here]

Shen et al.<sup>33</sup> also studied ZnO as a coating material. Unlike Dai's work, sol-gel method was used to prepare the AZO-coated LCO, which was believed to be more economically adoptable to battery applications. Moreover, Al element instead of Al<sub>2</sub>O<sub>3</sub> was introduced into the ZnO lattice replacing Zn partially. AZO layer was deposited evenly throughout the surface of LCO particles. The amount of AZO coating material was 0.5 wt%, 1 wt%, 2 wt% and 4 wt% of the LCO powder respectively. 2% AZO coating gave the best result for cycling performance test in which it maintain a capacity retention of 92.4% (173 mAh/g) after 200 cycles between 2.75 V and 4.5 V at a current density of 100 mA/g. The coated material also showed much better rate performance. Discharge capacity at the rate of 8C was 86.6% of that at 0.1C for 2% AZO coated LCO. The result for bare LCO at the rate of 8C was only 45.4% of that at 0.1C. The rate performance of 2% AZO coated LCO showed best result, delivering a reversible capacity of 156 mAh/g at 8C. It is believed that beside physical barrier and conductive networks, the AZO coating material also plays an important role of HF consumer, so that the surface structure is stabilized and excellent cycling capability is retained. From the two examples of modified ZnO coating material, it is concluded that doping Al<sub>2</sub>O<sub>3</sub> or Al could improve the conductivity of the coating material, which provides the conductive network to decrease impedance and also act as a protection layer. However, the amount of the coating material (the thickness of the coating layer) affects the electrochemical performance of the material by blocking lithium ion transportation when too thick layer is coated. It is important to find a balance.

As SiO<sub>2</sub> has a particular thermal property and it provides a scavenging effect for the hydrogen fluoride (HF) which is a common product of the reaction between residual water and LiPF<sub>6</sub> salt in the electrolyte, it is often chosen as the coating material for Ni-rich cathode material such as NCM622<sup>40</sup> and NCM523<sup>41</sup>, because in these materials, the high nickel content causes cell performance degradation over time due to side reactions such as dissolution of metal from the cathode into the electrolyte, solid electrolyte interface (SEI). And the degradations are greatly accelerated at elevated temperature. By coating nano-sized SiO<sub>2</sub> onto NCM622, Cho et al. found out that the thermal stability of the coated material was improved. The main exothermic peak of decomposition of the charged electrode at 4.3V shifted from 275 °C to 288 °C and the related heat generation was decreased from 1882 J/g to 1217 J/g thanks to the high thermal stability of SiO<sub>2</sub>. The SiO<sub>2</sub> coating can suppress the decomposition of electrolyte at the contact surface with electrode which triggers the oxygen generation from NCM. As a result, the cycle performance of the electrode at high temperature is improved. The SiO<sub>2</sub> also shows ability of HF scavenging, which benefit the capacity retention. In Cho et al.'s experiment, an electrolyte containing 1000 ppm of water was used to create an environment where HF could be generated by the reaction between water and LiPF<sub>6</sub>. The coated material maintained a 92% capacity retention after 2 cycles at 0.1 C and 48 cycles at 1C, whereas the pristine NCM was able to maintain 68% of the capacity.

In another example of SiO<sub>2</sub> coating, Chen et al.<sup>41</sup> coated SiO<sub>2</sub> on NCM 523 via wet chemistry method and found out similar results that 0.5 wt% SiO<sub>2</sub>-coated sample showed higher capacity retentions and better

cycling stability even at a high cut-off voltage and a high current density. The result of the experiment also indicated that the SiO<sub>2</sub> coating layer with suitable amount of silica could enhance the Li<sup>+</sup> diffusion rate at the interface of electrode and electrolyte during cycling. The amount of transition metal dissolved in the electrolyte was analyzed by ICP and it was found out that the amount of SiO<sub>2</sub>-coated sample dissolved in the electrolyte is lower than that of the pristine sample. So it showed that SiO<sub>2</sub> may suppress the transition metal dissolution and the silica layer could protect active material from HF attack. The thermal stability of the material was also improved, the pristine material had an exothermic peak at 436 °C and the reaction released heat of 278.7 J/g whereas the coated sample had a higher peak at 442 °C and less heat was released (171.5 J/g). This illustrated that SiO<sub>2</sub> coating layer reduced heat generation and suppressed oxygen release.

Other oxides coating materials have also been studied. Cao et al.<sup>42</sup> studied Al<sub>2</sub>O<sub>3</sub> coated NCM523 and found out that the coated material had high reversible capacity, good cycling stability and better rate capability compared to the bare NCM because Al<sub>2</sub>O<sub>3</sub> coating layer could suppress the oxygen elimination, prevent the HF corrosion and reduce interface impedance. Hildebrand et al.<sup>43</sup> compared the effects of Al<sub>2</sub>O<sub>3</sub>, SiO<sub>2</sub> and TiO<sub>2</sub> coated NCA cathode material and concluded that all these coating materials improved thermal stability. However, the overall capacity was decreased due to their additional inactive mass. Min et al.<sup>44</sup> coated Co<sub>3</sub>O<sub>4</sub> on LiNi<sub>0.91</sub>Co<sub>0.06</sub>Mn<sub>0.03</sub>O<sub>2</sub>. In fact, the Co<sub>3</sub>O<sub>4</sub> is reactive with Li residue on the material surface forming a layer of LiCoO<sub>2</sub>. The coated NCM exhibited superior capacity retention and rate capability compared to bare material. Different oxides can result in quite different electrochemical properties of the cathode materials upon coating due to their unique chemical and physical properties. However, the general role of coating material is to provide a physical barrier between the electrode and electrolyte to prevent undesired reactions.

### 3.1.2 Li<sup>+</sup> conducting coating materials

Lithium salt is another kind of coating material, some of which can also be considered as active electrode materials, such as LFP<sup>45</sup>, LTO<sup>46</sup> and Li<sub>2</sub>SiO<sub>3</sub> (inactive material)<sup>47,48</sup>. Lithium salts, compared with the above-mentioned oxides and fluorides, have a unique advantage that can be described as high Li<sup>+</sup> ion conduction. Meng et al.<sup>49</sup> coated NCM811 with Li<sub>2</sub>TiO<sub>3</sub> by coating TiO<sub>2</sub> onto NCM hydroxide precursor and lithiating the material through physical grounding. The weight ratio of Li<sub>2</sub>TiO<sub>3</sub> to NCM was 3 wt%. It was found out that Li<sub>2</sub>TiO<sub>3</sub> coating layer could suppress the decomposition of LiPF<sub>6</sub> in the electrolyte. The surface of the coated cathode comprised more organic decomposition products, which was beneficial to the transmission of Li ions through the cathode surface. Li<sub>2</sub>TiO<sub>3</sub> was also beneficial to stabilize the structure of NCM material. Compared to the bare reference material, the coated cathode maintained an integrated morphology after 170 cycles as shown in Figure 7.

[Figure 6 here]

$\text{Li}_4\text{Ti}_5\text{O}_{12}$  is a ternary Li-Ti-O oxide, of which the zero-strain characteristic can ensure high structural stability and fast Li ion diffusion during cycling.<sup>46</sup> Zhang et al. coated this material on NCM523 through a solid state synthesis process using  $\text{TiO}_2$  and  $\text{CH}_3\text{COOLi}$ . Additionally,  $\text{Li}_7\text{Ti}_5\text{O}_{12}$  was converted from  $\text{Li}_4\text{Ti}_5\text{O}_{12}$  during cycling, which collectively provided good electronic and Li ion conductivity. Among the series of samples, 1.0 wt% LTO coated NCM523 exhibited the best electrochemical performance. The LTO coating layer served as both a Li ion conductive layer and a protective layer, improving the structure stability and electronic diffusion. A capacity retention of 91% was achieved after 100 cycles at cutoff voltages of 4.5 V. Meanwhile, the coated material also showed an improved thermal stability at 60 °C.

Compared to  $\text{SiO}_2$  coating material,  $\text{Li}_2\text{SiO}_3$  is such a material which not only stabilizes the structure of the bulk cathode materials but also provides high Li ion conduction.<sup>47,48</sup> Two groups of researchers (Hu et al. and Zhao et al.) coated  $\text{Li}_2\text{SiO}_3$  on NCM523 and NCM811. They found out that the coating material had largely improved the Li ion diffusion rate and reduced the charge transfer resistance of the electrode. The cycling performance and rate capability have also been enhanced.

$\text{Li}_2\text{ZrO}_3$  is a lithium ion conductive material which can be coated on layered cathode materials such as LCO<sup>32</sup> and NCM<sup>50</sup>. Like previously mentioned  $\text{Li}_4\text{Ti}_5\text{O}_{12}$ ,  $\text{Li}_2\text{ZrO}_3$  can provide low strain path for lithium ion diffusion, which can improve high-rate performance of the material. In Zhang et al.'s work,  $\text{Li}_2\text{ZrO}_3$  was coated on LCO via a synchronous lithiation route. In this synthesis route, the coating material and cathode active material were produced by lithiation of the precursor  $\text{ZrO}_2$  coated  $\text{CoC}_2\text{O}_4 \cdot x\text{H}_2\text{O}$  (cobalt oxalate). The synthesis is illustrated in Figure 8 below. The  $\text{ZrO}_2$  coating procedure was realized by the reaction between the crystal water released from  $\text{CoC}_2\text{O}_4 \cdot 2\text{H}_2\text{O}$  and  $\text{Zr}(\text{OC}_4\text{H}_9)_4$ .

[Figure 7 here]

The as-prepared cathode material was confirmed to be a single-phased layered structure with a space group of  $\text{R}\bar{3}\text{m}$  by XRD. The lattice parameter *c* showed an obvious increase which indicated that  $\text{Zr}^{4+}$  had also been incorporated into the bulk structure. As a result of  $\text{Li}_2\text{ZrO}_3$  coating, the capacity retention of the material was largely improved even at both room temperature and an elevated temperature of 55 °C. The specific capacity at 10 C has also been significantly increased from 33.9 mAh/g to 103mAh/g. The coating material has been acting as a protective layer which inhibited the side reaction and transition metal dissolution. Meanwhile, lithium ion diffusion and electronic conductivity was improved. As a result, the cycle performance, rate capability and thermal stability of the coated material achieved a large improvement.

Liang et al. coated  $\text{Li}_2\text{ZrO}_3$  on NCM811 via a similar synthesis route by lithiation of the Zr material coated precursor. The coated material exhibited an improved cycle performance and rate performance. 2%  $\text{Li}_2\text{ZrO}_3$  coated sample was able to achieve a capacity retention of 94.5% after 200 cycles. It must be noted that 1% coating sample had a higher capacity than the 2% sample after 200 cycles even though the latter sample's

capacity retention was higher because the initial discharge capacity difference caused by the different amount of inactive coating material used. 1%  $\text{Li}_2\text{ZrO}_3$  sample show superior high rate capability compared with bare and other amount samples. Again, the amount of coating material plays an important role in balancing between protection, sacrifice of active material and electrochemical performance as the previous samples have illustrated.

Besides the above-mentioned coating materials, there are also some others that are quite interesting. Polypyrrole (PPy)<sup>34</sup>, metals<sup>51</sup>, etc. are among these coating materials. Core-shell structured cathode materials could also be considered as coated materials. In core-shell materials, the particles are manufactured in two phases, first a core of high capacity material that is usually high nickel such as NCM811, and then on top of this a layer of more stable material such as NCM111 is precipitated. This prevents the high nickel phase from reacting with electrolyte and supports the particle surface, which is the most likely to be over drained from its lithium content during charge. Core-shell materials are another huge branch of research centered around improving the stability of cathodes, so they are not discussed here in more detail.<sup>52</sup>

### 3.2 Doping

The most important goal of doping layered cathode materials is to improve stability of the cathode in its delithiated state. During charging, Li-ions are removed from the layer structure, leaving vacancies between the  $\text{MeO}_6$  layers (Figure 9). As more and more Li ions are removed, the metal oxide layers will start to repulse each other more and more because of similar charge. At some level of lithium removal, the situation becomes energetically untenable, metal ions from the transition metal layer will start to migrate into the lithium layer. The atoms will rearrange to form spinel or rock salt structure instead of layer structure, releasing the “extra” oxygen that is over stoichiometric for the spinel structure. This rearrangement is irreversible and therefore ruins the battery. More importantly, this rearrangement is accompanied by release of oxygen and heat, so it is quite dangerous as well.<sup>54</sup> In addition to over-charge, rise in temperature can trigger this cathode structure rearrangement, and cathode materials temperature resistance is directly affected by the degree of lithium removal. Higher voltage (higher degree of lithium removal) means that battery is more vulnerable to thermal runaway.

[Figure 8 close here]

Because of this instability in delithiated state, the whole theoretical capacity of cathode can never be utilized, only certain percentage of Li-ions can be removed safely. As can be seen in Table 1 (in the beginning of modification methods section), the differences in capacities of layered cathode materials are not due to theoretical capacity differences, but are instead related to the fraction of Li-ions that can be removed from the material during charging. For unmodified NCM333 this is about 70% of Li-ions which limits the safe upper voltage limit to about 4.4 V vs Li.<sup>55</sup> For LCO the percentage of Li that can be safely removed is 50%, which corresponds to about 4.2 V.<sup>56</sup>

Dopants act loosely speaking as support struts, they are electrochemically inactive components that make the layer structure more resistant to changes. This means that larger portion of the theoretical capacity can be used, safely. Other effects to consider when doping are speed of Li-ion diffusion, cation mixing, oxidation potentials and lattice volume changes. Often the amount of dopant needs to be carefully optimized because a small amount can improve structural stability, but a large amount starts to inhibit Li-ion diffusion. Some dopants are able to inhibit cation mixing, which means transition metal atoms moving from their intended place to the lithium layer. Cation mixing is in itself an unwanted phenomenon as it prevents battery from functioning optimally<sup>57</sup>, but is also linked to easier oxygen release from the material. Oxidation potentials determine to the operating voltage of the battery. Dopants that can lessen the lattice changes will prevent microcracking and improve cycle life. Larger c-parameter will also increase Li-ion diffusion speed in the structure.<sup>57</sup> Large amounts of dopant are always unwanted, because most dopants don't contribute to the electrochemical activity, and therefore doped materials generally have lower initial discharge capacity.

The list of dopants that have been investigated includes, but is not limited to Na, K, Mg, Al, Ti, Cu, Cr, Ga, Fe, Zn, Sn, Mo, Zr, W, Nb,  $\text{SO}_4^{2-}$ ,  $\text{PO}_4^{3-}$  and  $\text{F}^-$ . To make sense of this plethora of substances, the vague concept of “doping” needs to be divided to several different categories. Doping methods can be divided to late-stage doping and doping during precursor manufacturing. Dopants can be divided in to three categories based on where they attach in the structure. The first group forms a solid solution with the transition metal, i.e. takes the place of Me in  $\text{MeO}_6$  octahedra. The second group intercalates to  $\text{Li}^+$  sites instead. The third group are anionic dopants, which replace O-atoms.

### 3.2.1 Doping methods

Doping can be divided in to two different types depending on at which point of manufacturing it is done. More common and easier to achieve, is doping during precursor heat treatment (oxidation and lithiation). Typically this “late-stage” doping is done as simply as mixing the precursor in a mechanical mixer with the wanted dopant, and then heating the mixture in an oven somewhere around 500-1000 °C.<sup>58-60</sup> Doping in such a late stage usually gives very uneven depth-distribution of the dopant, because only the surface of the particles comes in touch with the dopant, though for example Li et al.<sup>61</sup> report uniform cross-section distribution of dopant during lithiation phase using a hydrothermal process. In some cases it is unclear whether an improvement in electrochemical behavior is actually achieved by doping, or if the effect comes just from having a coating layer on the particles. Sampling depth of XRD, for example, is too deep to notice a thin coating layer.

The second sort of doping is precursor doping during manufacturing. Most commonly this means co-precipitation, adding the wanted dopant in the reactor while precursor is being precipitated,<sup>62,63</sup> though there are other manufacturing methods where doping can be done simultaneously, such as sol-gel method<sup>64</sup> and self-combustion.<sup>65</sup> All of these methods begin with aqueous metal solutions, which puts a lot of restrictions on the doping element. The dopant needs to have a salt that is at least somewhat soluble in a solvent that can

be added to the reactor without ruining the product, and it needs to precipitate in the same conditions as the precursor. Doping during manufacturing gives a very even distribution of the dopant throughout the precursor particles. This means that there are no concentration gradients in the material and there is less strain on the particle because it behaves similarly throughout.

Anion doping is done very similarly to cation doping, but usually in late stage. It involves mechanically mixing the precursor with a reactant salt either in solid state<sup>66</sup> or in solvent<sup>67</sup>.

### 3.2.2 Solid solution dopants

These dopants are intended to form a solid solution with the main cathode material, preserving the layered  $\alpha$ -NaFeO<sub>2</sub> structure. This means that the doping metal occupies an identical position in the MeO<sub>6</sub> octahedra as Co atom would in LCO. Usually transition metals are used, but other metals can be incorporated in to the structure also. The list of all these metals is quite long, and for ease of notation, battery scientists seem to have reappropriated the term “transition metal” to refer to all of these metals, including aluminium, magnesium and tin. Most of these dopants work by the same mechanisms, they improve the strength of the Me-O bonds (leading to improved structural stability) and stop cation disordering by physically blocking the path of transition metal moving to lithium position. The effects of a dopant depend on its size (most transition metal ions are about the same size) and valence electrons (there will be charge balance reactions between the different transition metal ions in order to have them at stable oxidation states so that the energy of the system is minimized). A complete detailed discussion of all the studied dopants would be very long, so the below section includes detailed information of only some common ones.

One of the best studied dopants is aluminium. Aluminium is cheap, abundant and nontoxic. Al has also been successfully doped into the precursor during precipitation, so industrial manufacturing of evenly Al doped cathodes is possible. LiAlO<sub>2</sub> by itself has  $\alpha$ -NaFeO<sub>2</sub> structure, but is not electrochemically active because the intercalated Li-ions can not be easily removed (i.e. a battery made with LiAlO<sub>2</sub> can not be charged).<sup>68</sup> Instead it has been of interest as a dopant from late 90s. Al is in the structure as Al<sup>3+</sup>. It has been shown to counteract the instability of delithiated structure in most layer structured cathodes, even composite cathodes<sup>69</sup>, and as a result Al doping can improve both safety and lifetime of a LIB. DFT calculations show that it is energetically favorable for Al<sup>3+</sup> to form a solid solution with the transition metals in NCM structure, preserving a layered structure instead of forming a new phase. The structural stability improvement appears to be due to the strong Al-O bonds, which inhibit structural changes in the MeO<sub>6</sub> octahedra.<sup>70</sup> During deep charge Al<sup>3+</sup> also migrates preferentially and is stable in a tetrahedral site in the lithium layer. This blocks other metal atoms from moving in to the tetrahedral position, and from there to an octahedral position in the lithium layer, which is the mechanism of layered structure transforming in to spinel structure. The transformation of layer to spinel structure releases oxygen, so preventing or slowing this reaction improves safety.<sup>71</sup> Calculations by Ceder et al.<sup>68</sup> and experimental data by Jang et al.<sup>72</sup> of Al doping in to LCO and LiNiO<sub>2</sub><sup>73</sup> indicate that Al doping raises the Li-ion intercalation potential. This means that the operating voltage of the battery needs to be higher in

order to utilize the same capacity as in undoped cathode. This rise is proportional to the amount of doped Al. Jang et al. report that around 50% of Co in LCO can be replaced by Al, but stability improvements were not observed by raising the doping amount above 25%. 25% Al doping reduced lattice variation during cycling almost by half and was able to prevent layered to spinel transformation on cycling between 2,5-4,4V, although particle strain was still observed. Al doped  $\text{LiNiO}_2$  also had a smaller degree of cation mixing. Al doping shrinks the a lattice parameter (assumed to be due to shortening of Me-O bonds) and lengthens the c parameter (longer interlayer distance). Unfortunately, Al in the  $\text{MeO}_6$  also hinders Li-ion mobility<sup>70</sup>, so its amount needs to be carefully optimized. Usually the amount of added Al is no more than 5%, because further increase will hinder rate performance. Al as a dopant also does not contribute to charge of the battery so it is lost capacity.

Another cheap, abundant and nontoxic dopant is iron, and it can also be doped in via co-precipitation method. There are somewhat discordant results about the benefits of Fe doping. There seems to be no benefit in replacing Co with Fe. Fe is in the structure as  $\text{Fe}^{3+}$ . Holtzapfel et al.<sup>74</sup> found that large amount of Fe (20%) in LCO dropped initial discharge capacity (cycled to 4,4 V) by half and over 40% started to give very broad peaks in XRD, indicating loss of well-ordered structure. Liu et al.<sup>75</sup> doped NCM333 with increasing amounts of Fe replacing Co, and compared it to Al replacing Co. Their results (also cycled to 4,4 V) indicate that Fe doping is not equally beneficial as Al doping, both dopants slightly lowering the initial discharge capacity, but the 5% Al doped sample was the only one showing equal or better cycling behavior as undoped sample.

Fe doping makes the lattice parameters c and a longer, presumably because the  $\text{Fe}^{3+}$  has larger ionic radius than  $\text{Co}^{3+}$ . There is another consideration to iron doping that is not a worry with Al doping: A study by Alcántara et al.<sup>76</sup> found that iron in LCO, even at low levels (0,5%) tends to cluster and these clusters distort the layer structure in such a way that Li-ion diffusion is severely affected. This effect was lessened by proper heat treatment (850 °C) which prevented Fe clustering. Fe doped in to LCO can also induce cation mixing (Fe in Li sites). This effect was lessened with excess lithium during lithiation. There might be some benefit to Fe doping above 4,4 V. Calculations show that when charged to voltages over 4,4 V, Fe could oxidize from 3+ to 4+, and therefore contribute to the capacity. The cycle life is however low. Li et al. studied co-precipitated iron doped NCM333, with 5% of Ni replaced by Fe.<sup>77</sup> Iron doping was shown to suppress cation mixing effectively. Cell cycled between 2,5 – 4,5 V at 0,5 C had initial discharge capacity of 146 mAh/g and retained 87,3% of capacity after 50 cycles. Undoped comparison sample had initial discharge capacity of 131 mAh/g and had capacity retention of 86,7% after 50 cycles. More importantly, the capacity loss for the doped sample happened mostly during the first five cycles after which the capacity loss was slow, but the undoped sample lost capacity at a constant rate.

Ramesha et al.<sup>78</sup> studied  $\text{Li}_{1,2}\text{Ni}_{0,13}\text{Co}_{0,13}\text{Mn}_{0,54-x}\text{M}_x\text{O}_2$  doped with Co, Fe and Cr replacing Mn. The best stability and cycling improvements were observed with 10% added cobalt. 10% Cr also showed similar or slightly better performance. Fe doped sample showed similar or worse performance compared to pristine sample, but was able to suppress oxygen release.

Mohan et al.<sup>64</sup> doped Cr in to NiO<sub>2</sub> by sol-gel method. Cr was shown to be incorporated in to the layered structure. Cr increased c- lattice and decreased a- parameter (interpreted as strengthened metal bonds). 10% Cr substitution gave better initial capacity (204 mAh/g) than non-doped sample (194 mAh/g) and capacity retention after 50 cycles (95% vs. 92%). Increasing the Cr amount further started to decrease capacity and cyclability. Cr has many oxidation levels, so it would be good dopant if it was electrochemically active, though these results indicated that it was not participating. Also chromium is about as toxic as cobalt, so as a cobalt replacement it is not ideal.

Tin is a very promising dopant candidate. Eilers-Rethwisch et al.<sup>62</sup> compared NCM622 doped with Al, Fe and Sn by co-precipitation method. Al and Fe were shown to be incorporated in to the layered structure without forming a new phase. Tin mostly formed a solid solution, though there were signs of possible second phase, which however did not seem to be detrimental to the battery. When cycled between 2,5 – 4,3 V at 1 C, the undoped comparison sample NCM622 showed better capacity (~20 mAh/g) but dropped down to SOH 80% faster than the undoped samples. Sn doped NCM622 had the biggest improvement, about 20% longer cycling time until SOH 80%. The structural stability improvements were confirmed in TG and DSC measurements, where all doped samples improved temperature resistance, but Sn doped sample gave 50 % less mass loss until 650 °C and released only a fifth of the heat amount compared to undoped sample. Perhaps most interestingly Sn doped sample showed better performance at higher C rates than Fe or Al doped sample (though still worse than undoped sample) indicating that Sn does not inhibit Li-diffusion speed as severely as Al and Fe.

Wilcox et al.<sup>79</sup> compared NCM333 doped with Al, Fe and Ti replacing Co by self-combustion method. They also noticed that Fe doped materials suffer from structural problems and poor rate capability. They identified 8% Ti doped material as the best sample, because the initial capacity was same as the undoped materials. Ti doped sample also had better rate capability at high C-rates than undoped material, presumed to be because the inter-slab layer was widened, and when cycled between 2,0-4,7 V the Ti doped sample had better capacity retention than undoped sample. They speculated that replacing Co<sup>3+</sup> with Ti<sup>4+</sup> (so called aliovalent substitution because they have different valence states) will cause a charge compensation reaction where Mn<sup>4+</sup> is partially reduced to Mn<sup>3+</sup>. Mn<sup>3+</sup> oxidation back to Mn<sup>4+</sup> happens within 3-3,5V, which means that even though the added Ti is electrochemically inactive, it will be compensated for by the Mn that is made active.

Kam and Doeff<sup>80</sup> studied Ti doping in to NCM333 further. They found based on XRD diffraction patterns that the Ti amount can only be increased to about 7% before a second phase starts to form. Best performance was gained with 2% Ti doping. When charged to 4,3 V the initial discharge capacity (196 mAh/g) was slightly better than undoped (184 mAh/g). Cycling between 2,0-4,7 V the 2 and 3 % Ti doped samples had significantly higher capacities and better capacity retention than undoped sample.

As stated, this is not a complete list of dopants. Other dopants include Zr<sup>81</sup>, which is also found to be a beneficial dopant, but hard to be doped in during manufacturing, Ga<sup>82</sup>, some rare metals, etc.

### 3.2.3 Li site dopants

Some dopants intercalate in to lithium positions instead of inhabiting transition metal positions. Such dopants are low oxidation number cations such as K<sup>59</sup>.

Elements intercalating in to Li sites can affect the interlayer distance. Because Li is so small, replacing it with Na or K, leads to widening of the interlayer distance. This widening leads to faster Li-diffusion speed. But if the amount of dopant is too large, the effect is the opposite, hindering Li diffusion and because they are not electrochemically active, reducing capacity and large amounts are very bad for battery performance. 1-3% seems to be somewhat optimal.<sup>59</sup>

With LLOs there are some studies that have achieved improved material characteristics by replacing the Li in the transition metal layer. This is different from replacing lithium in the lithium layer, but still included under Li site dopant. Sallard et al.<sup>83</sup> studied substitution of Li<sup>+</sup> by Mg<sup>2+</sup> in the transition metal layer in Li-rich NCM. They found that 1% Mg substitution exhibits lower voltage drop and more stable structure during cycling than unsubstituted material. However, substitution of 2,5% or more resulted in higher voltage drop during cycling, due to the faster formation of the spinel like structure.

### 3.2.4 Anion doping

Anion doping means substituting oxygen with another anion. Similar structure stabilizing effects can be achieved with anion doping as cation doping, but unlike cationic dopants, anion dopant does not take the place of an electrochemically active species. The list of elements that can be substituted for oxygen is much shorter than the ones that can be substituted for transition metals. Basically they are halogens F<sup>-</sup>, Cl<sup>-</sup>, Br<sup>-</sup> and elements that can form polyanions with oxygen such as BO<sub>3</sub><sup>3-</sup> / BO<sub>4</sub><sup>5-</sup>, SO<sub>4</sub><sup>2-</sup> and PO<sub>4</sub><sup>3-</sup>. Anion doping with for example fluoride has been known to improve cathode performance for decades but has seen little commercial use. Recently LLOs have raised a new interest towards anionic dopants. Mechanisms of anion doping involve complicated orbital energy level changes, and the effects that different anions have cannot be easily predicted. DFT calculations are a valuable tool in evaluating possible materials.

Kim et al.<sup>84</sup> studied F<sup>-</sup>-doping to NCM333 during lithiation and found that doped F<sup>-</sup> amount could be raised to 15% before another phase started to form. Their results also indicated that the good effects could be achieved with only a small amount of F-doping (~5%). Increasing amount of F<sup>-</sup> doping increased both a and c lattice parameters. The strong Li-F bond was speculated to be the reason for this, as it could increase repulsion in the oxygen layer. The strong Li-F bond was also suspected to be the reason for drop in initial capacity (Li-ions harder to remove) and improvement in cycle life when cycled up to 4,6 V (layer structure more stable when some Li remains in the structure). All fluorinated samples (5, 10 and 15%) showed also

improved rate capability, so much that at 1 C all the doped samples had better efficiency than undoped sample. Doped samples also had better thermal resistance and safety in DSC measurements.

Yan et al.<sup>85</sup> used DFT calculations to investigate halogen doping in to nickel based LLO. They found that Cl doping could improve stability, rate performance and lower the voltage needed to fully charge the material. In contrast, F doping could raise the needed voltage, and Br doping could lead to formation of a second phase.

Li et al.<sup>86</sup> doped boracic acid in to high Mn LLO with sol-gel method to make a material with the chemical formula of  $\text{Li}_{1,2}\text{Ni}_{0,13}\text{Co}_{0,13}\text{Mn}_{0,54}(\text{BO}_4)_{0,75x}(\text{BO}_3)_{0,25x}\text{O}_{2-3,75x}$ . Doped material showed initial capacity of 319 mAh/g when cycled to 4,6 V at 0,1 C and capacity retention of 89% after 300 cycles, which is good for LLO. The doping also increased the materials thermal resistance. Better stability is attributed to the lessened covalent nature of M-O bonds, which in very simplified terms means that Co atoms will participate more in the redox rather than shift all of the electron vacancies on oxygen atoms. This helps reduce the amount of  $\text{O}^{2-}$  oxidizing to  $\text{O}_2$  gas and preserves the structure.

#### 4. Conclusions

There are several ways in which the qualities of layered cathode materials may still be fine-tuned. Table 2 lists some modified materials in no particular order. The situation with conventional LIBs is starting to move from needing cathode materials with better energy capacity to needing electrolytes that can handle higher voltages so that all the capacity can be used.

[Table 2 here]

The price of cobalt is still a major problem, because the layered materials with best stability all have some cobalt in the structure. The demand for all sorts of rechargeable battery systems is growing, so the price is unlikely to come down any time soon. It is likely that there will not be one universal LIB cathode material, instead big stationary applications will utilize cheaper but less energy dense spinel materials ( $\text{LiFePO}_4$  and  $\text{LiMn}_2\text{O}_4$ ) and the volume and weight sensitive applications such as EVs and laptops and cellphones will continue to use layered mixed metal oxide materials.

#### References

1. M Stanley Whittingham. *Chemical Reviews*, 2004, **104**(10), 4271-4302.
2. K. Mizushima, P. C. Jones, P. J. Wiseman and J. B. Goodenough. *Materials Research Bulletin*, 1980, **15**(6), 783-789.

3. M. M. Doeff. Battery cathodes in *Batteries for sustainability*. ed. R.J. Brodd, 1. Aufl. ed. Springer-Verlag, New York, NY, 2013.
4. T. Ohzuku, Y. Makimura. *Chem Lett*, 2001, **30**(7), 642-643.
5. X. Wang, X. Zheng, Y. Liao, et al. *Journal of Power Sources*, 2017, **338**, 108-116.
6. A. Basch, L. de Campo, J. H. Albering and J. W. White. *Journal of Solid State Chemistry*, 2014, **220**, 102-110.
7. R. Fallahzadeh, N. Farhadian. *Solid State Ionics*, 2015, **280**, 10-17.
8. Hu G, Du K, Peng Z. *Cathode materials for lithium ion batteries: Principle, performance and production technology*. Beijing: Beijing Industrial Publisher; 2017:103-133.
9. N. Nitta, F. Wu, J. T. Lee and G. Yushin. *Materials Today*, 2015, **18**(5), 252-264.
10. M. Dixit, M. Kosa, O. S. Lavi, B. Markovsky, D. Aurbach and D. T. Major. *Physical chemistry chemical physics : PCCP*, 2016, **18**(9), 6799.
11. J. Li, L. Wang, Q. Zhang and X. He. *Journal of Power Sources*, 2009, **189**(1), 28-33.
12. M. Kim, H. Shin, D. Shin and Y. Sun. *Journal of Power Sources*, 2006, **159**(2), 1328-1333.
13. J. W. Fergus. *J Power Sources*, 2010, **195**(4), 939-954.
14. H. Wang, H. He, N. Zhou, G. Jin and Y. Tang. *Transactions of Nonferrous Metals Society of China*, 2014, **24**(2), 415-422.
15. C. H. Chen, J. Liu, M. E. Stoll, G. Henriksen, D. R. Vissers and K. Amine. *J Power Sources*, 2004, **128**(2), 278-285.
16. K. A. Jarvis, Z. Deng, L. F. Allard, A. Manthiram and P. J. Ferreira. *Chemistry of Materials*, 2011, **23**(16), 3614-3621.

17. J. M. Paulsen, C. M. Thomas and J. R. Dahn. *Journal of The Electrochemical Society*, 2000, **147**(3), 861.
18. Z. Lu, D. D. MacNeil and J. R. Dahn. *Electrochem Solid State Letters*, 2001, **4**(11), A194.
19. E. Shinova, E. Zhecheva, R. Stoyanova and G. D. Bromiley. *Journal of Solid State Chemistry*, 2005, **178**(5), 1661-1669.
20. M. M. Thackeray, S. Kang, C. S. Johnson, J. T. Vaughey, R. Benedek and S. A. Hackney. *Journal of Materials Chemistry*, 2007, **17**(30), 3112.
21. G. Assat, J. Tarascon. *Nature energy*, 2018, **3**, 373.
22. J. Xu, M. Sun, R. Qiao, et al. *Nat Commun*, 2018, **9**(1), 1-10.
23. K. Kleiner, B. Strehle, A. R. Baker, et al. *Chem Mater*, 2018, **30**(11), 3656-3667.
24. M. Lang, M. S. D. Darma, K. Kleiner, et al. *Journal of Power Sources*, 2016, **326**, 397-409.
25. S. B. Chikkannanavar, D. M. Bernardi and L. Liu. *Journal of Power Sources*, 2014, **248**, 91-100.
26. A. G. Ritchie, C. O. Giwa, J. C. Lee, et al. *Journal of Power Sources*, 1999, **80**(1), 98-102.
27. K. C. Kam, M. M. Doeff. *Material Matters*, 2012, **7**(4), 56.
28. Fetcenko M. BASF - ANL collaboration on NCM cathode materials. Updated 2014. Accessed 7.6., 2018.
29. D. R. Gallus, R. Schmitz, R. Wagner, et al. *Electrochimica Acta*, 2014, **134**(Supplement C), 393-398.
30. H. Zheng, Q. Sun, G. Liu, X. Song and V. S. Battaglia. *Journal of Power Sources*, 2012, **207**(Supplement C), 134-140.
31. M. Wohlfahrt-Mehrens, C. Vogler and J. Garche. *Journal of Power Sources*, 2004, **127**(1), 58-64.

32. J. Zhang, R. Gao, L. Sun, H. Zhang, Z. Hu and X. Liu. *Electrochimica Acta*, 2016, **209**, 102-110.
33. B. Shen, P. Zuo, Q. Li, et al. *Electrochimica Acta*, 2017, **224**, 96-104.
34. D. Wang, X. Li, Z. Wang, H. Guo, Y. Xu and Y. Fan. *Electrochimica Acta*, 2016, **196**, 101-109.
35. X. He, C. Du, B. Shen, et al. *Electrochimica Acta*, 2017, **236**, 273-279.
36. D. Zuo, G. Tian, X. Li, D. Chen and K. Shu. *Journal of Alloys and Compounds*, 2017, **706**, 24-40.
37. R. Zhao, J. Liang, J. Huang, et al. *Journal of Alloys and Compounds*, 2017, **724**, 1109-1116.
38. X. Dai, A. Zhou, J. Xu, B. Yang, L. Wang and J. Li. *Journal of Power Sources*, 2015, **298**, 114-122.
39. S. Liu, Z. Wang, Y. Huang, et al. *Journal of Alloys and Compounds*, 2018, **731**, 636-645.
40. W. Cho, S. Kim, J. H. Song, et al. *Journal of Power Sources*, 2015, **282**, 45-50.
41. C. Chen, T. Tao, W. Qi, et al. *Journal of Alloys and Compounds*, 2017, **709**, 708-716.
42. Z. Cao, Y. Li, M. Shi, et al. *Journal of The Electrochemical Society*, 2017, **164**(2), A481.
43. S. Hildebrand, C. Vollmer, M. Winter and F. M. Schappacher. *Journal of The Electrochemical Society*, 2017, **164**(9), A2198.
44. K. Min, K. Park, S. Y. Park, S. Seo, B. Choi and E. Cho. *Journal of The Electrochemical Society*, 2018, **165**(2), A85.
45. S. -. Kim, K. J. Lee, W. J. Choi, et al. *Journal of Solid State Electrochemistry*, 2010, **14**(6), 919-922.
46. M. Zhang, G. Hu, L. Wu, Z. Peng, K. Du and Y. Cao. *Electrochimica Acta*, 2017, **232**, 80-88.
47. G. Hu, M. Zhang, L. Wu, Z. Peng, K. Du and Y. Cao. *Journal of Alloys and Compounds*, 2017, **690**, 589-597.
48. E. Zhao, M. Chen, Z. Hu, D. Chen, L. Yang and X. Xiao. *Journal of Power Sources*, 2017, **343**, 345-353.

49. K. Meng, Z. Wang, H. Guo, X. Li and D. Wang. *Electrochimica Acta*, 2016, **211**, 822-831.
50. H. Liang, Z. Wang, H. Guo, J. Wang and J. Leng. *Applied Surface Science*, 2017, **423**, 1045-1053.
51. A. Tornheim, V. A. Maroni, M. He, D. J. Gosztola and Z. Zhang. *Journal of The Electrochemical Society*, 2017, **164**(13), A3005.
52. P. Hou, H. Zhang, Z. Zi, L. Zhang and X. Xu. *J. Mater. Chem. A*, 2017, **5**(9), 4254-4279.
53. J. Shi, D. Xiao, X. Zhang, et al. *Nano Res*, 2017, **10**(12), 4201-4209.
54. S. Bak, K. Nam, W. Chang, et al. *Chemistry of Materials*, 2013, **25**(3), 337-351.
55. S. -. Yin, Y. -. Rho, I. Swainson and L. F. Nazar. *Chemistry of Materials*, 2006, **18**(7), 1901-1910.
56. G. G. Amatucci, J. M. Tarascon and L. C. Klein. *Solid State Ionics*, 1996, **83**(1), 167-173.
57. K. Kang, G. Ceder. *Phys Rev B*, 2006, **74**(9), 094105.
58. A. H. Tavakoli, H. Kondo, Y. Ukyo and A. Navrotsky. *Journal of the Electrochemical Society*, 2012, **160**(2), A305.
59. Y. Sun, L. Zhang, Y. Zhou, et al. *journal of the electrochemical society*, 2018, **165**(2), A338.
60. Y. Zhang, Z. Wang, J. Lei, et al. *Ceramics International*, 2015, **41**(7), 9069-9077.
61. L. Li, Y. Li, P. Li, et al. *Ceramics International*, 2017, **43**(4), 3483-3488.
62. M. Eilers-Rethwisch, M. Winter and F. M. Schappacher. *Journal of Power Sources*, 2018, **387**, 101-107.
63. D. Aurbach, O. Srur-Lavi, C. Ghanty, et al. *Journal of the Electrochemical Society*, 2015, **162**(6), A1027.
64. P. Mohan, K. Kumar, G. Kalaignan and V. Muralidharan. *J Solid State Electrochem*, 2012, **16**(12), 3695-3702.

65. W. El Mofid, S. Ivanov, A. Konkin and A. Bund. *Journal of Power Sources*, 2014, **268**, 414-422.
66. K. Kubo, M. Fujiwara, S. Yamada, S. Arai and M. Kanda. *J Power Sources*, 1997, **68**(2), 553-557.
67. S. Han, J. H. Song, T. Yim, Y. Kim, J. Yu and S. Yoon. *Journal of The Electrochemical Society*, 2016, **163**(5), A750.
68. M. K. Aydinol, D. R. Sadoway, Y. -. Jang, B. Huang, G. Ceder and Y. -. Chiang. *Nature*, 1998, **392**(6677), 694-696.
69. B. Seteni, N. Rapulenyane, J. C. Ngila and H. Luo. *Materials Today: Proceedings*, 2018, **5**(4, Part 2), 10479-10487.
70. M. Dixit, B. Markovsky, D. Aurbach and D. T. Major. *Journal of The Electrochemical Society*, 2017, **164**(1), A6365.
71. M. Guilmard, L. Croguennec, D. Denux and C. Delmas. *Chemistry of Materials*, 2003, **15**(23), 4476-4483.
72. Y. Jang, B. Huang, H. Wang, et al. *J Electrochem Soc*, 1999, **146**(3), 862-868.
73. Y. Jang, B. Huang, H. Wang, et al. *Journal of Power Sources*, 1999, **81**, 589-593.
74. M. Holzapfel, R. Schreiner and A. Ott. *Electrochimica Acta*, 2001, **46**(7), 1063-1070.
75. D. Liu, Z. Wang and L. Chen. *Electrochimica Acta*, 2006, **51**(20), 4199-4203.
76. R. Alcántara, G. Ortiz, J. L. Tirado, R. Stoyanova, E. Zhecheva and S. Ivanova. *J Power Sources*, 2009, **194**(1), 494-501.
77. L. Hongjian, G. Chen, B. Zhang and J. Xu. *Solid State Communications*, 2008, **146**, 115.
78. K. Ramesha, R. N. Ramesha and C. P. Laisa. *Electrochimica Acta*, 2017, **249**, 377-386.
79. J. Wilcox, S. Patoux and M. Doeff. *J Electrochem Soc*, 2009, **156**(3), A198.

80. K. C. Kam, M. M. Doeff. *J Mater Chem*, 2011, **21**(27), 9991-9993.
81. S. H. Oh, S. M. Lee, W. I. Cho and B. W. Cho. *Electrochim Acta*, 2006, **51**(18), 3637-3644.
82. R. Stoyanova, E. Zhecheva, G. Bromiley, et al. *J Mater Chem*, 2002, **12**(8), 2501-2506.
83. S. Sallard, D. Sheptyakov and C. Villevieille. *Journal of Power Sources*, 2017, **359**, 27-36.
84. G. Kim, M. Kim, S. Myung and Y. K. Sun. *Journal of Power Sources*, 2005, **146**(1), 602-605.
85. H. Yan, B. Li, Z. Yu, W. Chu and D. Xia. *J Phys Chem C*, 2017, **121**(13), 7155-7163.
86. B. Li, H. Yan, J. Ma, et al. *Adv Funct Mater*, 2014, **24**(32), 5112-5118.
87. B. Guo, J. Zhao, X. Fan, et al. *Electrochimica Acta*, 2017, **236**, 171-179.
88. H. Zhu, T. Xie, Z. Chen, et al. *Electrochimica Acta*, 2014, **135**, 77-85.
89. Z. Huang, Z. Wang, X. Zheng, et al. *Electrochimica Acta*, 2015, **182**, 795-802.
90. C. P. Laisa, R. N. Ramesha and K. Ramesha. *Electrochimica Acta*, 2017, **256**, 10-18.

## Table Captions

**Table 1** Theoretical and practical capacities of different cathode materials.

**Table 2** Capacities of doped cathode materials.

## Figure Captions

**Figure 1** Layered structure of LCO. All layered cathode materials share a similar structure with only minor variations to lattice parameter lengths. (Reprinted from Ref 6. Journal of Solid State Chemistry., 220, A. Basch, L. de Campo, J. H. Albering and J. W. White, Chemical delithiation and exfoliation of  $\text{Li}_x\text{CoO}_2$ , Pages 102-110, Copyright 2014, with permission from Elsevier.)

**Figure 2** Battery performance vs. nickel content.

**Figure 3** Lithium rich layered oxide structure is crystallographically different (C2/m) from traditional layered oxides (R-3m), but still has distinct lithium layers and metal oxide layers with lithium. Li-ions in the Li-layer behave similarly to traditional materials. Work is being done to determine whether the Li-ions in metal oxide layers can be reversibly intercalated.

(Reprinted (adapted) from Ref 16. Chemistry of Materials 23(16). Karalee A. Jarvis, Zengqiang Deng, Lawrence F. Allard, et al, Atomic Structure of a Lithium-Rich Layered Oxide Material for Lithium-Ion Batteries: Evidence of a Solid Solution, Pages 3614-3621, Copyright 2011, with permissions from American Chemical Society.)

**Figure 4** Specific discharge capacity of two full cells made with the same unmodified NCM622 cathode during cycling between 3.0-4.2 V.

**Figure 5.** Cycling performance of the bare and AZO-coated LCO electrodes tested between 3.0 V and 4.5 V at 0.2 C: (a) reversible discharge capacity for 50 cycles; (b) AZO thickness dependence of the capacity retention after 50 cycles. (Reprinted (adapted) from Ref 38. Journal of Power Sources 298. X. Dai, A. Zhou, J. Xu, B. Yang, L. Wang and J. Li., Superior electrochemical performance of  $\text{LiCoO}_2$  electrodes enabled by conductive  $\text{Al}_2\text{O}_3$ -doped ZnO coating via magnetron sputtering, Pages 114-122, Copyright 2015, with permissions from Elsevier)

**Figure 6** Comparison of Bare and  $\text{Li}_2\text{TiO}_3$  Coated NCM after 170 cycles. (bare NCM on the left and coated NCM on the right).

(Reprinted (adapted) from Ref 49. Electrochimica Acta 211. K. Meng, Z. Wang, H. Guo, X. Li and D. Wang. Improving the cycling performance of  $\text{LiNi}_{0.8}\text{Co}_{0.1}\text{Mn}_{0.1}\text{O}_2$  by surface coating with  $\text{Li}_2\text{TiO}_3$ , Pages 822-831, Copyright 2016, with permissions from Elsevier)

**Figure 7.** Synthesis of  $\text{Li}_2\text{ZrO}_3$  Coated LCO

**Figure 1.** Li-vacancies and cation mixing in the Li-layer. (Reprinted (adapted) from Ref 53. Nano Res 10(12). J. Shi, D. Xiao, X. Zhang, et al., Improving the structural stability of Li-rich cathode materials via reservation of cations in the Li-slab for Li-ion batteries, Pages 4201-4209, Copyright 2017, with permissions from Tsinghua University Press and Springer-Verlag Berlin Heidelberg)

Table 1. Theoretical and practical capacities of different cathode materials

Material	Theoretical capacity (mAh/g)	Practical capacity (mAh/g)	% of Li reversibly removed	Source
LiCoO <sub>2</sub>	274	142	52	26
LiNiO <sub>2</sub>	275	145	53	26
LiMnO <sub>2</sub> (layered)	286	Converts to spinel during cycling		26
LiMn <sub>2</sub> O <sub>4</sub> (spinel)	148	120	81	26
LiNi <sub>0.8</sub> Co <sub>0.2</sub> O <sub>2</sub>	274	180	66	26
LiNi <sub>0.8</sub> Co <sub>0.15</sub> Al <sub>0.05</sub> O <sub>2</sub>	279	180-200	65-72	27
LiNi <sub>1/3</sub> Co <sub>1/3</sub> Mn <sub>1/3</sub> O <sub>2</sub>	278	160-170	56-61	27
LiFePO <sub>4</sub>	170	170	100	27
NCM333	278	154	55	28
NCM523	278	164	59	28
NCM424	279	155	56	28
NCM622	277	178	64	28
NCM811	276	>185	>67	28
Mn-rich He-NCM		260		28

Table 2. Capacities of doped cathode materials

Material	Doping method	Cycling voltage (V)	Initial discharge capacity (mAh/g)	Capacity retention (%)	Cycles	C-rate	Source
LiNi <sub>0.6</sub> Mn <sub>0.2</sub> Co <sub>0.15</sub> Al <sub>0.05</sub> O <sub>2</sub>	coprecipitation	2.5 - 4.3	145	80	140	1	62
LiNi <sub>0.6</sub> Mn <sub>0.2</sub> Co <sub>0.15</sub> Sn <sub>0.05</sub> O <sub>2</sub>	coprecipitation	2.5 - 4.3	160	80	155	1	62
LiNi <sub>0.6</sub> Mn <sub>0.2</sub> Co <sub>0.15</sub> Fe <sub>0.05</sub> O <sub>2</sub>	coprecipitation	2.5 - 4.3	156	80	148	1	62
LiGa <sub>0.05</sub> Co <sub>0.95</sub> O <sub>2</sub>	high-pressure	3.0 - 4.7	215		1	0.02	82
LiGa <sub>0.1</sub> Co <sub>0.9</sub> O <sub>2</sub>	high-pressure	3.0 - 5.0	197		1	0.02	82
LiGa <sub>0.25</sub> Co <sub>0.75</sub> O <sub>2</sub>	high-pressure	3.0 - 5.1	132		1	0.02	82
Li(Ni <sub>0.5</sub> Co <sub>0.2</sub> Mn <sub>0.3</sub> ) <sub>0.99</sub> Mo <sub>0.01</sub> O <sub>2</sub>	hydrothermal	2.5 - 4.5	154	97	50	8	61
0.01% Al-LiNi <sub>0.5</sub> Co <sub>0.2</sub> Mn <sub>0.3</sub> O <sub>2</sub>		3.0 - 4.3	168		50	0.07	63
Li <sub>1.2</sub> Ni <sub>0.13</sub> Co <sub>0.13-x</sub> Mn <sub>0.54</sub> Al <sub>x</sub> O <sub>2(1-y)</sub> F <sub>2y</sub>	coprecipitation	3.0 - 4.5	250	88.2	150	0.5	87
LiAl <sub>y</sub> Co <sub>1-y</sub> O <sub>2</sub> (y=0-0.5)	coprecipitation	2.0 - 4.4	182	61	9	0.125	72
LiCo <sub>1-x</sub> Fe <sub>x</sub> O <sub>2</sub> (x=0.2)	solid reaction	3.0 - 4.4	164	43	2	0.025	74
LiCo <sub>0.995</sub> Fe <sub>0.005</sub> O <sub>2</sub>	re-anneal	3.2 - 4.3	143	87	50	0.1	76
Li <sub>1.2</sub> Ni <sub>0.13</sub> Co <sub>0.13</sub> Mn <sub>0.44</sub> Cr <sub>0.1</sub> O <sub>2</sub>	sol-gel	2.0 - 4.8	224	93.7	50	0.1	78
Li <sub>1.2</sub> Ni <sub>0.13</sub> Co <sub>0.13</sub> Mn <sub>0.49</sub> Fe <sub>0.05</sub> O <sub>2</sub>	sol-gel	2.0 - 4.8	230	90.4	50	0.1	78
Li <sub>1.2</sub> Ni <sub>0.13</sub> Co <sub>0.23</sub> Mn <sub>0.44</sub> O <sub>2</sub>	sol-gel	2.0 - 4.8	248	88.8	50	0.1	78
LiCr <sub>0.1</sub> Ni <sub>0.9</sub> O <sub>2</sub>	sol-gel	3.0 - 4.5	185	95.1	50	0.5	64
LiCr <sub>0.2</sub> Ni <sub>0.8</sub> O <sub>2</sub>	sol-gel	3.0 - 4.5	155	90.3	50	0.5	64
LiNi <sub>0.6</sub> Mn <sub>0.2</sub> Co <sub>0.15</sub> Al <sub>0.025</sub> Fe <sub>0.025</sub> O <sub>2</sub>	selfcombustion	2.5 - 4.4	189	89.9	10	0.05	65
Li <sub>1.08</sub> Ni <sub>0.92</sub> O <sub>1.9</sub> F <sub>0.1</sub>	solid reaction	3.0 - 4.3	200	63	100	1	66
Li(Ni <sub>0.5</sub> Co <sub>0.2</sub> Mn <sub>0.3</sub> ) <sub>0.97</sub> V <sub>0.03</sub> O <sub>2</sub>	solid reaction	2.7 - 4.4	170.5	88.5	50	1	88
LiNi <sub>0.59</sub> Co <sub>0.2</sub> Mn <sub>0.2</sub> Mg <sub>0.01</sub> O <sub>2</sub>	coprecipitation	2.8 - 4.3	177.1	90.0	100	1	89
		2.8 - 4.5	179.7	87.7	100	1	89
Li <sub>1.19</sub> Ca <sub>0.005</sub> Ni <sub>0.13</sub> Co <sub>0.13</sub> Mn <sub>0.54</sub> O <sub>2</sub>	sol-gel	2.0 - 4.8	273	82.5	100	0.2	90

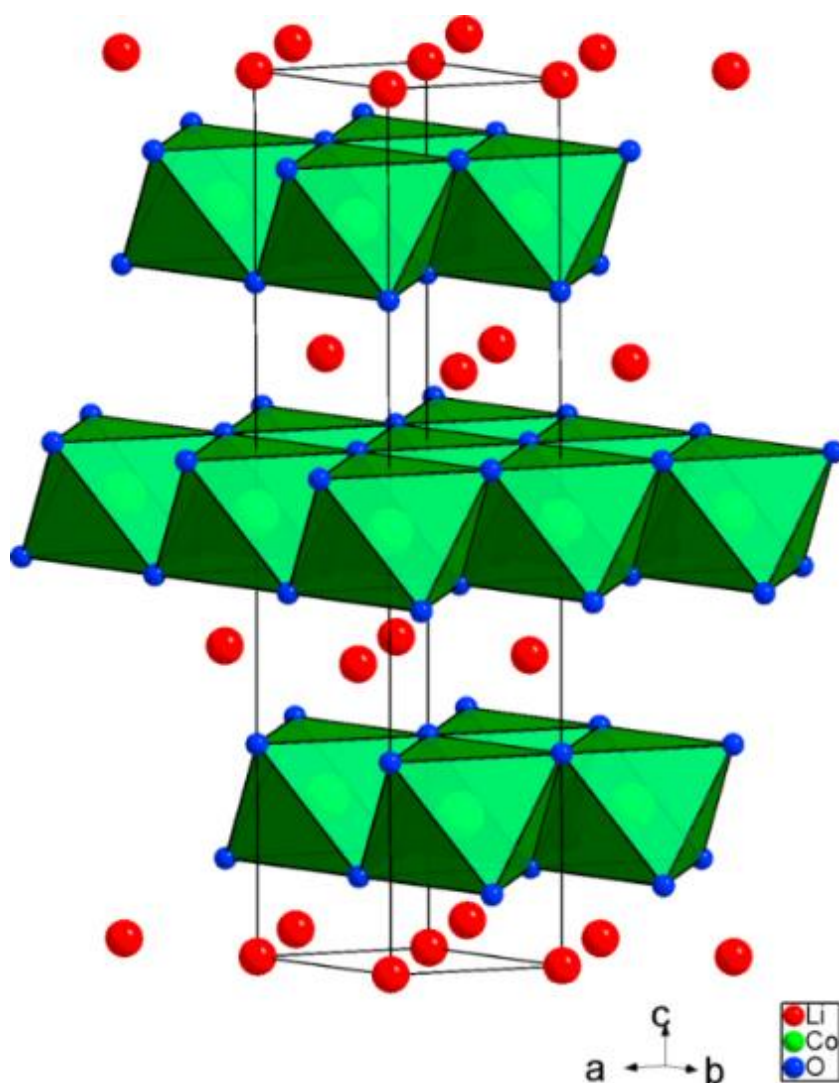


Figure 2 Layered structure of LCO. All layered cathode materials share a similar structure with only minor variations to lattice parameter lengths.

(Reprinted from Ref 6. Journal of Solid State Chemistry., 220, A. Basch, L. de Campo, J. H. Albering and J. W. White, Chemical delithiation and exfoliation of  $\text{Li}_x\text{CoO}_2$ , Pages 102-110, Copyright 2014, with permission from Elsevier.)

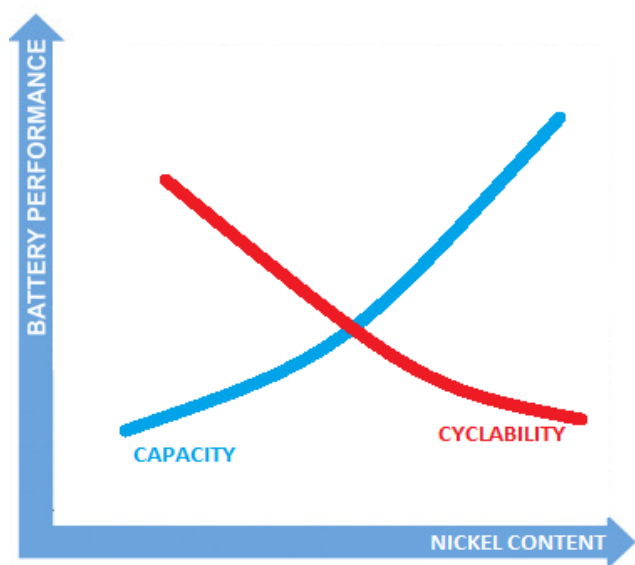


Figure 3. Battery Performance vs. Nickel Content

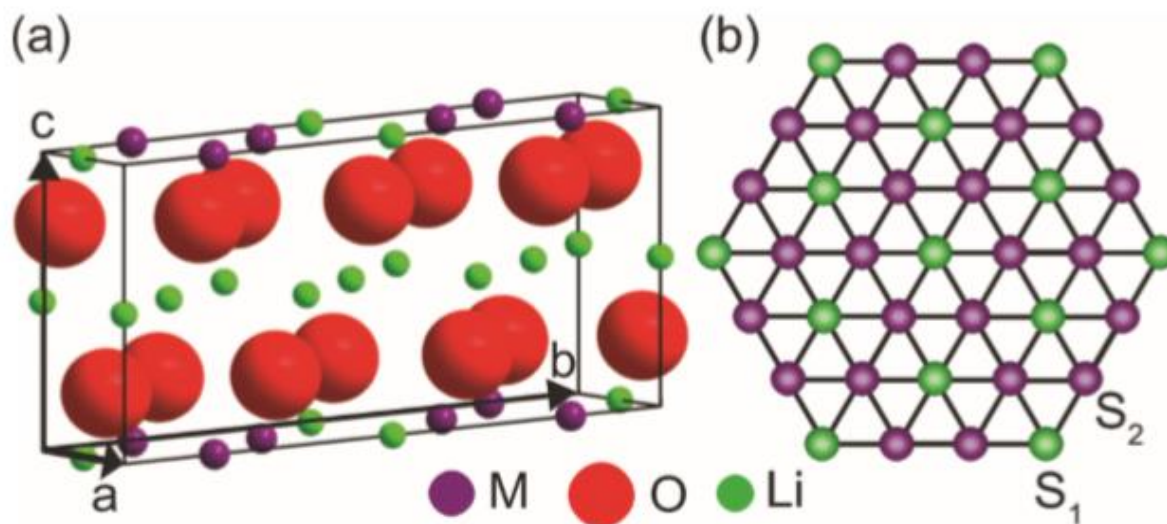


Figure 4 Lithium rich layered oxide structure is crystallographically different ( $C2/m$ ) from traditional layered oxides ( $R-3m$ ), but still has distinct lithium layers and metal oxide layers with lithium. Li-ions in the Li-layer behave similarly to traditional materials. Work is being done to determine whether the Li-ions in metal oxide layers can be reversibly intercalated.

"Reprinted (adapted) from Ref 16. Chemistry of Materials 23(16). Karalee A. Jarvis, Zengqiang Deng, Lawrence F. Allard, et al, Atomic Structure of a Lithium-Rich Layered Oxide Material for Lithium-Ion Batteries: Evidence of a Solid Solution, Pages 3614-3621, Copyright 2011, with permissions from American Chemical Society."

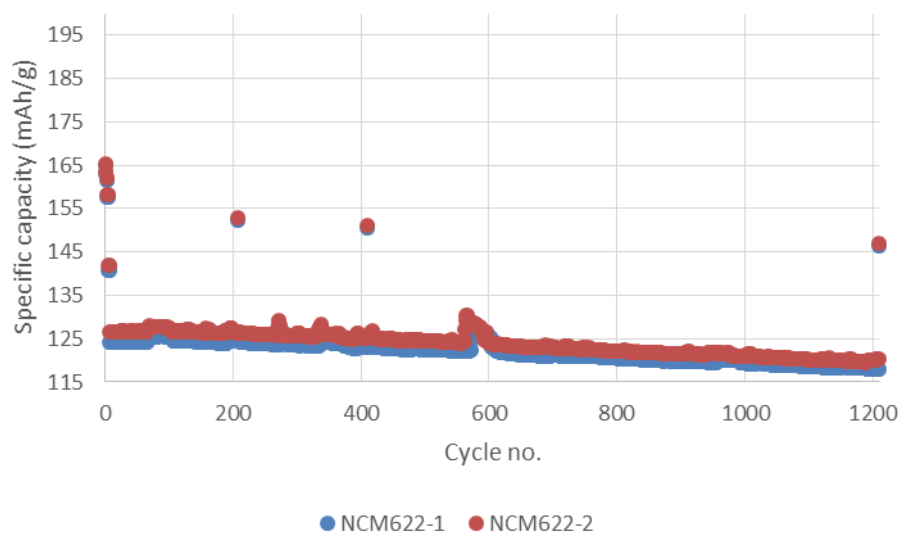


Figure 5 Specific discharge capacity of two full cells made with the same unmodified NCM622 cathode during cycling between 3,0-4,2 V.

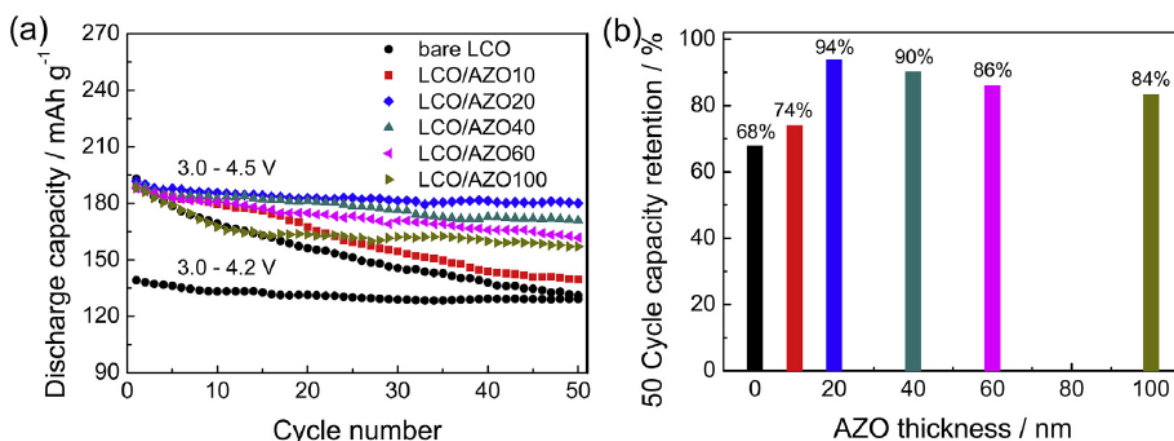


Figure 6. Cycling performance of the bare and AZO-coated LCO electrodes tested between 3.0 V and 4.5 V at 0.2 C: (a) reversible discharge capacity for 50 cycles; (b) AZO thickness dependence of the capacity retention after 50 cycles.

(Reprinted (adapted) from Ref 38. Journal of Power Sources 298. X. Dai, A. Zhou, J. Xu, B. Yang, L. Wang and J. Li., Superior electrochemical performance of  $\text{LiCoO}_2$  electrodes enabled by conductive  $\text{Al}_2\text{O}_3$ -doped ZnO coating via magnetron sputtering, Pages 114-122, Copyright 2015, with permissions from Elsevier)

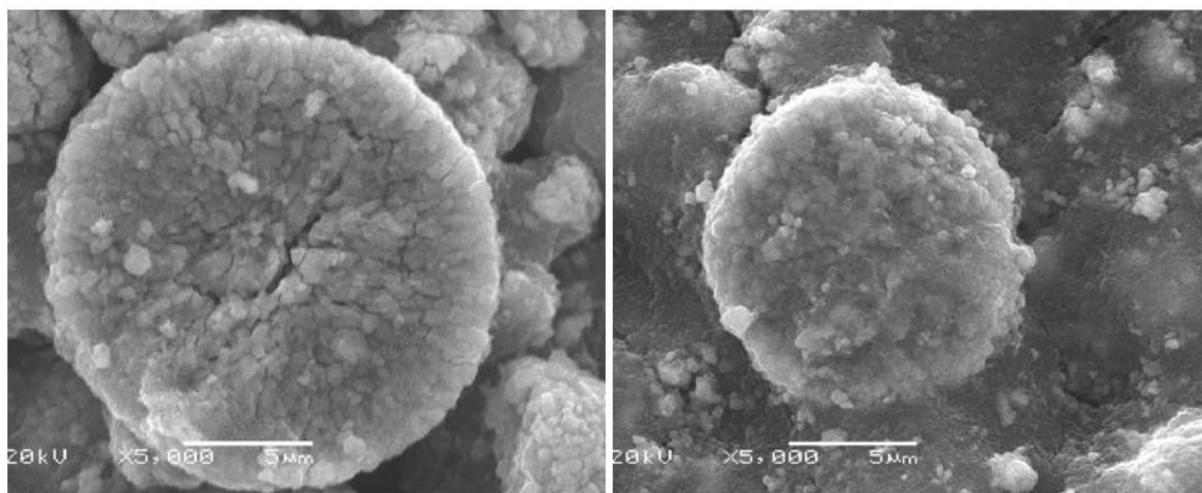


Figure 7. Comparison of Bare and  $\text{Li}_2\text{TiO}_3$  Coated NCM after 170 cycles. (bare NCM on the left and coated NCM on the right).

(Reprinted (adapted) from Ref 49. *Electrochimica Acta* 211. K. Meng, Z. Wang, H. Guo, X. Li and D. Wang. Improving the cycling performance of  $\text{LiNi}_{0.8}\text{Co}_{0.1}\text{Mn}_{0.1}\text{O}_2$  by surface coating with  $\text{Li}_2\text{TiO}_3$ , Pages **822-831**, Copyright 2016, with permissions from Elsevier)

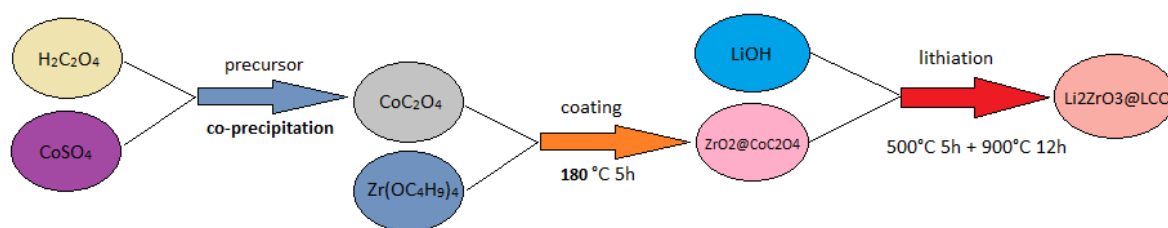


Figure 8. Synthesis of  $\text{Li}_2\text{ZrO}_3$  Coated LCO

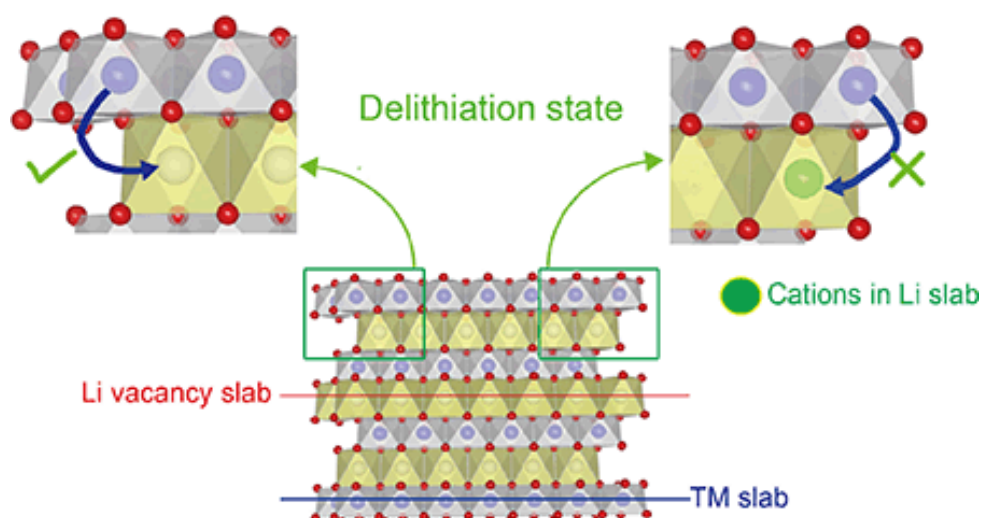


Figure 9 Li-vacancies and cation mixing in the Li-layer.

(Reprinted (adapted) from Ref 53. Nano Res 10(12). J. Shi, D. Xiao, X. Zhang, et al., Improving the structural stability of Li-rich cathode materials via reservation of cations in the Li-slab for Li-ion batteries, Pages 4201-4209, Copyright 2017, with permissions from Tsinghua University Press and Springer-Verlag Berlin Heidelberg)